

# Nuclear astrophysics studies with $4\pi$ BaF<sub>2</sub> calorimeters

F. Käppeler, M. Heil, and R. Plag  
*Forschungszentrum Karlsruhe, Institut für Kernphysik,  
 P.O. Box 3640, D-76021 Karlsruhe, Germany*

Recibido el 23 de enero de 2005; aceptado el 4 de marzo de 2005

The origin of the chemical elements in nucleosynthesis processes in stars and stellar explosions has been intensely investigated after these concepts were formulated in 1957 by Burbidge *et al.* [1]. It turned out that the abundances produced by the slow neutron capture process (*s* process) in the He burning zones of Red Giant stars, which contributes about half of the isotopic abundances in the mass region between Fe and Bi, could be quantitatively described on the basis of laboratory measurements. For obtaining the required accuracy, a  $4\pi$  BaF<sub>2</sub> array was developed and extensively used at Forschungszentrum Karlsruhe for measuring neutron capture cross sections in the relevant neutron energy range from 3 keV to 220 keV. Meanwhile, similar arrays have been built in Los Alamos and at CERN, and are now starting to produce data over wider neutron energy intervals. Recently it has been shown that such detector arrays are also perfectly suited for measuring stellar cross sections of charged particle induced reactions. The performance of these detectors is illustrated at the example of recent measurements followed by a discussion of possible future applications.

*Keywords:* Stellar nucleosynthesis; *s*-process; neutron capture; gamma calorimeter; charged particle reactions.

El origen de los elementos químicos en procesos de nucleosíntesis en estrellas y explosiones estelares ha sido investigado ampliamente desde que fueron formulados en 1957 por Burbidge *et al.* [1]. Resulta que la abundancia producida por el proceso de captura de neutrones lentos (proceso *s*) en las zonas de quemado de He en las estrellas rojas gigantes, las cuales contribuyen aproximadamente con la mitad de las abundancias isotópicas en la región con masas entre Fe y Bi, puede ser descrita de forma cuantitativa con base en los experimentos de laboratorio. Para obtener la exactitud requerida, se desarrolló un arreglo de BaF<sub>2</sub> de  $4\pi$ , el cual ha sido usado en Centro de Karlsruhe para medir la sección eficaz de captura de neutrones en el rango energético del neutrón de 3 KeV a 220 keV. De igual forma se han construido arreglos en Los Alamos y en el CERN, por lo que ahora se están obteniendo datos en intervalos de energía del neutrón muy amplios. Recientemente se ha mostrado que los detectores mencionados son también muy adecuados para medir la sección eficaz estelar de reacción inducida por partículas cargadas. Se presentan las medidas más recientes como un ejemplo que ilustra el desempeño de esos detectores y se discute las aplicaciones futuras posibles.

*Descriptor:* Nucleosíntesis estelar; proceso *s*; captura neutrónica; calorímetro gama; reacciones con partículas cargadas.

PACS: 25.40.Lw; 29.40.Vj; 97.10.Cv

## 1. Introduction

This contribution deals with the application of large BaF<sub>2</sub> detector arrays in measurements of reaction rates for stellar He burning and the related nucleosynthesis aspects. Though the motivation for such measurements will be sketched and the implications of some results will be discussed, the reader is referred to the literature for a more comprehensive description of the astrophysical background. In particular, review articles dealing with the nuclear physics aspects of *s*-process nucleosynthesis [2–4] or with the stellar models for the astrophysical site of the *s* process and the corresponding astronomical observations [5] can be of interest.

Stellar models are aiming at an increasingly quantitative picture of stellar and galactic evolution and nucleosynthesis. To a large extent, the credibility of such models depends on how well they are reproducing the abundance patterns found in nature, e.g. the solar abundance distribution [6], the surface composition of Red Giant stars [7], and the isotope ratios in presolar grains [8]. This stellar model aspect, however, depends strongly on the quality of the underlying nuclear physics data, which must be determined in laboratory experiments.

Presently, the best predictions can be made for the abundances produced during stellar He burning, where neutron capture nucleosynthesis in the slow neutron capture (*s*) pro-

cess takes place. Starting from this scenario, model predictions can not only be tested by comparison with the global abundance distribution but also in terms of the basic physical parameters at the *s*-process site, i.e. neutron density, temperature, and pressure, or with respect to the mixing mechanisms from the stellar interior to the surface.

In this context, reliable rates for neutron capture reactions along the *s*-process path are most crucial. The present status of the nuclear physics input for *s*-process nucleosynthesis and the remaining open problems are briefly sketched with emphasis on the need for rather accurate measurements. The second part deals with the progress achieved with large BaF<sub>2</sub> arrays coupled with various neutron sources. The immediate impact of accurate nuclear physics data on our understanding of the astrophysical *s*-process is illustrated by a few recent results.

## 2. STELLAR MODELS AND THE ROLE OF *s*-PROCESS BRANCHINGS

The following brief outline of stellar models for *s*-process nucleosynthesis indicates the main features and presents the concept of *s*-process branchings.

The schematic sketch of Fig. 1 shows the *s*-process path along the chart of nuclides. Since neutron capture times are typically of the order of one year, the reaction path follows

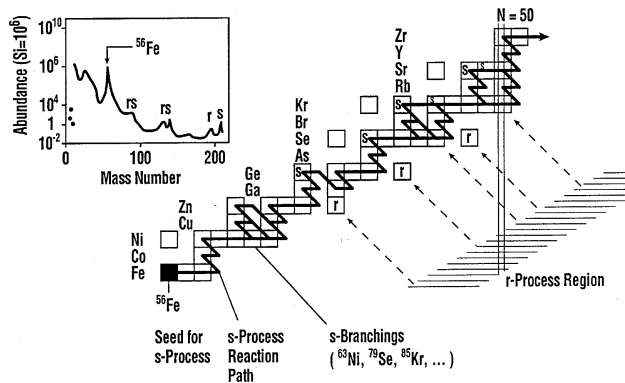


FIGURE 1. The neutron capture path of the  $s$  process along the stability valley. Isotopes marked by an "s" are shielded against beta decays from the  $r$ -process region. Apart from a minor  $p$ -process contribution, these nuclei are considered as  $s$ -only. The sharp  $s$ -process maxima in the observed abundance distribution (inset) result from the small cross sections of neutron magic nuclei.

the stability valley. An ensemble of about 35 isotopes can be considered to be of pure  $s$ -process origin, because they are shielded by stable isobars against beta decays from the  $r$ -process region. At some unstable nuclei, the reaction path splits into two branches due to competition between neutron capture and beta decay. The local abundance patterns resulting from these  $s$ -process branchings carry important information on the physical conditions during stellar He-burning.

The current  $s$ -process scenarios are thermally pulsing, low mass asymptotic giant branch (AGB) stars in the mass range between 1 and 3 solar masses ( $1 \leq M \leq 3M_{\odot}$ ) and massive stars with  $M \geq 8M_{\odot}$ . While the former are responsible for the main  $s$ -process component, i.e. the  $s$  abundances in the mass region between Zr and Bi [9], the latter are producing the weak  $s$  component, covering the mass range between the Fe group nuclei and Zr [10]. The underlying models were shown to describe the  $s$ -process part of the abundance distribution rather well, including the important isotope patterns of the various  $s$ -process branchings [5]. Neutron production occurs mainly via the  $^{13}\text{C}(\alpha, n)^{16}\text{O}$  reaction at a neutron density of about  $10^7 \text{ cm}^{-3}$ . This reaction provides 95% of the total neutron exposure in low mass AGB stars. The remaining 5% are contributed by the  $^{22}\text{Ne}(\alpha, n)^{25}\text{Mg}$  source at much higher neutron densities of up to  $10^{11} \text{ cm}^{-3}$ .

The  $s$  process in massive stars occurs during different evolutionary phases. First, neutrons are produced during core He burning by the  $^{22}\text{Ne}(\alpha, n)^{25}\text{Mg}$  reaction at temperatures of 300 MK ( $kT = 26 \text{ keV}$ ) and relatively low neutron densities of less than  $10^6 \text{ cm}^{-3}$ . Part of the material from this zone is exposed to a second neutron irradiation due to  $^{12}\text{C}(^{12}\text{C}, n)^{23}\text{Mg}$  reactions, which occur during the later carbon burning phase, when temperatures and neutron densities of 1 GK ( $kT = 91 \text{ keV}$ ) and  $10^{11} \text{ cm}^{-3}$  are reached, respectively.

The range of stellar  $s$ -process temperatures requires experimental neutron capture cross sections from about 300 eV

to several hundred keV. The measured  $(n, \gamma)$  cross sections,  $\sigma(E_n)$  have to be averaged over the thermal neutron spectra characteristic for the stellar sites. These Maxwellian averaged cross sections (MACS) are required for all nuclei from  $^{12}\text{C}$  up to  $^{209}\text{Bi}$ .

Though  $\beta$  decay is usually much faster than neutron capture, comparably long-lived isotopes in the  $s$ -process path give rise to branchings in the reaction path. This competition is expressed by a branching factor  $f_{\beta} = (\lambda_{\beta})/(\lambda_{\beta} + \lambda_n)$  that depends formally on the  $\beta$ -decay rate  $\lambda_{\beta} = \ln 2/t_{1/2}$  and on the neutron capture rate  $\lambda_n = n_n v_T \langle \sigma \rangle$  with  $n_n$  being the neutron density,  $v_T$  the mean thermal velocity, and  $\langle \sigma \rangle$  the MACS for the radioactive branch point nucleus. The  $s$ -process branchings produce a local abundance pattern that includes an  $s$ -only nucleus, which is partially bypassed by the reaction flow. Accordingly, these nuclei exhibit a smaller  $\langle \sigma \rangle N$  value than what is characteristic of the full reaction flow – and thus provide a measure for the strength of the branching. The different interplay between neutron capture and  $\beta$ -decay rates in the various branchings along the  $s$ -process path from Fe to Bi represents a viable and stringent test of  $s$ -process prescriptions and, hence, for models of the He burning phase of stellar evolution.

### 3. Stellar $(n, \gamma)$ rates – status and needs

Presently, experimental techniques for  $(n, \gamma)$  measurements have reached a stage where the 1% accuracy level required for sufficiently detailed analyses of particular abundance patterns can be met [11]. However, this level has been achieved so far only for a minority of the relevant isotopes. In addition to the remaining key nuclei, also a large number of cross sections with uncertainties in excess of 10% await improvement. In contrast to the fairly stable situation of the  $s$  process, explosive nucleosynthesis scenarios of the  $r$  and  $p$  processes imply complex reaction paths far from stability, which must be described by huge networks including several thousand reactions. By far most of these reaction rates have to be obtained by statistical model calculations [12, 13]. Nevertheless, experimental data for stable and as many unstable isotopes as possible are required for testing the necessary extrapolation to the region of unstable nuclei.

The main requests concentrate on  $(n, \gamma)$  measurements in the following areas:

- The cross sections of the key isotopes for  $s$ -process investigations should be determined with uncertainties of  $\approx 1\%$ . This goal has been reached only for half of the 33  $s$ -only nuclei between  $^{70}\text{Ge}$  and  $^{204}\text{Pb}$ .
- Meaningful analyses of the characteristic signatures preserved in presolar grains require also accurate cross sections with uncertainties of  $\approx 1\%$ . The present status is far from being adequate, particularly for the lighter elements, where about 70 isotopes are concerned.

- Nuclei at or near magic neutron numbers  $N=50$ ,  $82$ , and  $126$  act as bottlenecks for the reaction flow in the main  $s$ -process region between Fe and Bi. For the majority of these data the necessary uncertainties of  $\leq 3\%$  have not been reached.
- Though the final abundance patterns are shaped at  $kT = 23$  keV during the He shell flash the overall distribution is determined by the neutron exposure from the  $^{13}\text{C}(n,\alpha)^{16}\text{O}$  reaction, which operates at  $kT = 8$  keV. Reliable cross sections in the lower keV region are rather scarce and need significant improvement. This holds in particular for the neutron magic isotopes.
- Complementary investigations of competing reaction channels are needed for an improved assessment of SEF corrections.
- The cross sections of abundant light isotopes below Fe, which may constitute crucial neutron poisons for the  $s$ -process, need to be improved. Especially important are  $^{16}\text{O}$ ,  $^{18}\text{O}$ , and  $^{22}\text{Ne}$ .
- Cases where Direct Radiative Capture (DRC) contributes significantly to the astrophysical reaction rate are of particular interest, because this effect plays also an important role in  $r$ -process related, neutron-rich nuclei. Among the stable isotopes interesting examples are  $^{14}\text{C}$ ,  $^{16}\text{O}$ ,  $^{88}\text{Sr}$ ,  $^{138}\text{Ba}$ , and  $^{208}\text{Pb}$ .
- Nuclei, which still constitute white spots in the  $s$ -process chain or which exhibit very uncertain cross section, are found in the mass region below Fe, around  $A=100$ , and near the end of the  $s$ -process region. These gaps in the experimental data should be determined at the 5% level.
- Last, but not least, enhanced efforts should be directed to measurements on unstable nuclei. In addition to the activation technique, the very high neutron fluxes available at spallation neutron sources appear to be promising options for such studies. Priority should be given to the important branch points  $^{79}\text{Se}$ ,  $^{85}\text{Kr}$ ,  $^{147}\text{Pm}$ ,  $^{151}\text{Sm}$ ,  $^{163}\text{Ho}$ ,  $^{170}\text{Tm}$ ,  $^{171}\text{Tm}$ ,  $^{179}\text{Ta}$ ,  $^{204}\text{Tl}$ , and  $^{205}\text{Pb}$ .

Since neutron data for explosive nucleosynthesis are completely missing, any effort in this area provides a most useful support for amending the theoretically calculated rates. Neutron cross sections have a direct impact for scenarios with comparably low neutron densities as well as during the freeze-out phase of stellar explosions, where they contribute to flatten the pronounced odd-even effects predicted for the primary yields.

## 4. Neutron Capture Studies with $4\pi$ BaF<sub>2</sub> arrays

The best signature for the identification of neutron capture events is the total energy of the gamma cascade by which the product nucleus deexcites to its ground state. Hence, the accurate measurement of  $(n,\gamma)$  cross sections should use a detector that operates as a  $\gamma$ -ray calorimeter with good energy resolution. In the  $\gamma$  spectrum of such a detector, all capture events would fall in a line at the neutron separation energy (typically between 5 and 10 MeV), well separated from the  $\gamma$ -ray backgrounds that are inevitable in neutron experiments.

These arguments point to a  $4\pi$  detector of high efficiency, made of a scintillator with reasonably good time and energy resolution. In addition, this detector should be insensitive to scattered neutrons, since - on average - the scattering cross sections are about 10 times larger than the capture cross sections. The combination of these aspects is best achieved by a  $4\pi$  BaF<sub>2</sub> scintillation detector. Most important is the weak neutron sensitivity of BaF<sub>2</sub>, which keeps the background from scattered neutrons at a manageable level.

### 4.1. The Karlsruhe Detector

The concept of the Karlsruhe  $4\pi$  BaF<sub>2</sub> detector and the way it is operated is sketched in Fig. 2, showing the setup at the accelerator. The detector is indicated schematically by a computer simulation, which presents only the spherical BaF<sub>2</sub> shell (15 cm thickness and 20 cm inner diameter) consisting of 42 individual crystals, and the supporting structure. All other details are omitted for the sake of clarity.

Neutrons are produced by means of a pulsed Van de Graaff accelerator (repetition rate 250 kHz, average beam current  $2 \mu\text{A}$ , pulse width 0.7 ns) via the  $^7\text{Li}(p,n)^7\text{Be}$  reaction. The collimated neutron beam hits the sample in the centre of the detector at a flight path of 77 cm. Up to nine samples can be used in the measurements, all mounted on a vertical ladder. One position is occupied by a gold sample for determination of the neutron flux, while an empty sample position and a scattering sample are routinely used for background determination. The samples are cycled into the measuring position in intervals of about 10 min, which are defined by integrating the beam current on target. Additional

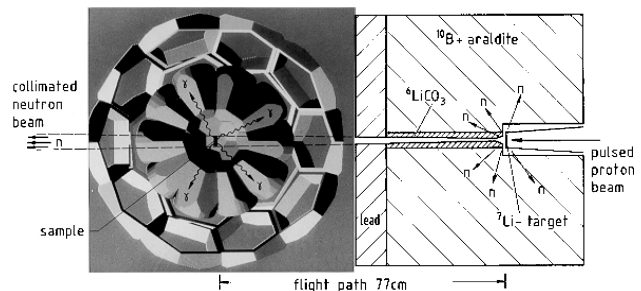


FIGURE 2. The Karlsruhe TOF setup with the  $4\pi$  BaF<sub>2</sub> array.

neutron monitors are used to check for equal neutron exposure per sample and to collect data for the correction of backgrounds due to scattered neutrons.

The essential features of the detector are: a resolution in gamma-ray energy ranging from 14% at 662 keV to 6% at 6.13 MeV, a time resolution of 500 ps, and an overall efficiency for capture events of about 96%. For a detailed description of the detector and of a typical measurement see Refs. [14, 15].

With this new detector, (n, $\gamma$ ) cross sections can be determined with an accuracy of 1 to 2%. The first measurement of the cross sections of the xenon isotopes 128, 129, and 130 at stellar neutron energies can be considered as a recent, typical example [16, 17]. This experiment has been performed on isotopically pure gas samples in the neutron energy range from 3 keV to 225 keV. Typically 300 mg to 600 mg of gas were contained in Ti spheres 10 mm in diameter and with 0.2 mm thick walls. The efficiency for capture events was evaluated by means of the experimental pulse height spectra shown in Fig. 3. Most of the events are, indeed, recorded in a line at the neutron separation energy. The tail towards lower energies corresponds to events where not all  $\gamma$ -rays of the cascade could be detected, mainly due to losses through the openings for the neutron beam and the sample changer.

A difficulty of this detector is, however, that neutrons are scattered from the sample in the center of the detector and are captured with about 10% probability by the Ba isotopes of the scintillator. This part of the background is difficult to distinguish from true capture events in the sample and must, therefore, be further reduced. In this respect, the comparably short flight path of the setup sketched in Fig. 2 has the advantage that the neutron flight times are rather short. Accordingly, interactions of neutrons scattered from the sample into the detector appear with a significant delay so that most of the corresponding background falls outside the TOF interval used for data analysis.

The fast timing provided by the short accelerator pulses and the excellent time resolution of the  $4\pi$  array results in an overall resolution in neutron energy of 1% at 30 keV. Fold-

ing the measured differential cross sections,  $\sigma(E_n)$ , with the stellar neutron spectra for various temperatures yields eventually the proper stellar values required for the description of *s*-process nucleosynthesis. In case of the xenon isotopes, the MACSs exhibit uncertainties of  $\sim 2\%$ , an order of magnitude smaller than reported before [11]. It is important to emphasize that this precision is indispensable for a meaningful discussion of the astrophysical information contained in the isotopic abundance ratios of the Xe isotopes [16, 17].

#### 4.2. BaF<sub>2</sub> Arrays at White Neutron Sources

Apart from the setup used at Karlsruhe, similar  $4\pi$  BaF<sub>2</sub> arrays have meanwhile also been installed at the spallation neutron sources LANSCE at Los Alamos [18] and at the n\_TOF facility at CERN [19] with the aim to cover a broader neutron energy range and to achieve higher sensitivity.

Spallation reactions induced by energetic particle beams constitute the most prolific pulsed sources of fast neutrons suited for TOF measurements. The main advantage of these facilities is the very efficient neutron production due to the high primary proton beam energies of 800 MeV and 20 GeV at LANSCE and n\_TOF, respectively. At n\_TOF, for example, a yield of 300 neutrons per incident proton is reached, which makes this facility the most luminous white neutron source presently available. By coupling the primary spallation targets with a moderator provides an energy spectrum that covers a wide range from thermal to GeV energies.

Due to their excellent efficiency spallation sources can be operated at low repetition rates while still maintaining high average intensities. The situation at LANSCE is characterized by a comparably short flight path of 20 m, a time resolution of 250 ns, and a repetition rate of 50 Hz - similar to what is planned at the SNS in Oak Ridge [20] and at J-PARC in Japan [21]. The new n\_TOF facility at CERN represents a complementary approach aiming at higher resolution (185 m flight path, 7 ns pulse width) and even lower repetition rates of typically 0.4 Hz [19].

Compared to the situation at the Karlsruhe Van de Graaff, the use of  $4\pi$  BaF<sub>2</sub> arrays at spallation sources implies more severe background problems due to scattered neutrons. Because of the continuous energy spectrum this background can no longer be reduced by TOF discrimination. Instead, neutron absorbers surrounding the sample are used to keep this problem under control. The best possible absorber material, which was chosen for the DANCE detector in Los Alamos [22], is <sup>6</sup>LiH due to the combined effect of the hydrogen (which acts as a moderator) and the <sup>6</sup>Li (which absorbs neutrons via the <sup>6</sup>Li(n,  $\alpha$ )<sup>3</sup>H reaction without producing any  $\gamma$ -rays). Moreover, <sup>6</sup>LiH has the least impact on the  $\gamma$ -ray spectrum of capture events because of its very low average atomic number.

An alternative solution had to be adopted for the  $4\pi$  BaF<sub>2</sub> detector at CERN in order to meet the site specific safety requirements. In this case, the lithium salt of the dodecanedioic acid (<sup>6</sup>LiOOC(CH<sub>2</sub>)<sub>10</sub>COO<sup>6</sup>Li) with isotopically

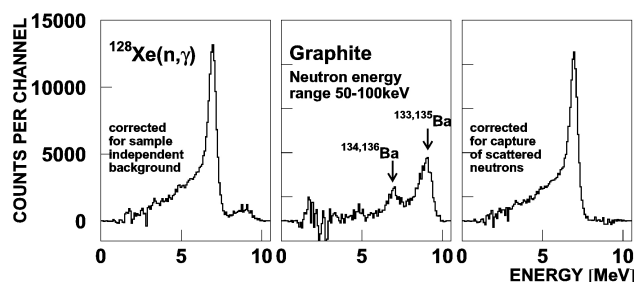


FIGURE 3. The  $\gamma$ -ray spectrum of keV neutron captures in <sup>128</sup>Xe shows that most events are recorded in a line at the binding energy of the captured neutron. Background subtraction due to capture of scattered neutrons is performed via the spectrum of a graphite sample (middle). The normalization factor is calculated to match the intensity around 9.2 MeV in both spectra. The corrected spectrum is plotted in the right part of the figure.

pure  ${}^6\text{Li}$  was used, an absorber material with acceptable neutron moderation and absorption efficiency and good  $\gamma$ -ray transmission [23]. Chemically, the compound is inert, non-inflammable, and suited for unlimited storage. In addition the  $\text{BaF}_2$  crystals were enclosed in 1 mm thick  ${}^{10}\text{B}$  loaded carbon fiber capsules to further enhance the neutron absorption effect.

The astrophysics options at various white neutron sources have been critically discussed by Koehler [24] with respect to measurements using radioactive samples. This comparison shows that spallation sources are unique for their peak neutron fluxes in the astrophysically relevant keV region, but that only the n\_TOF facility exhibits a neutron energy resolution comparable to that of electron linear accelerators. This comparison indicates that the n\_TOF facility would even allow for TOF measurements on sub-mg samples of radioactive isotopes if a 20 m flight path could be made available.

### 4.3. Future Options

Measurements of neutron capture cross sections of unstable isotopes via existing TOF techniques are restricted to samples with manageable specific activities. Therefore, samples with energetic decay  $\gamma$ -rays and with half-lives down to a few days are particularly challenging. Such investigations can only be imagined with a sufficiently sensitive technique that allows one to reduce the sample mass substantially. In fact, samples as small as a few micrograms are required in order to avoid prohibitive backgrounds from the decay of the sample itself.

A drastic improvement of the TOF technique to the point, where measurements can be carried out with microgram samples, was proposed recently [25]. This approach foresees a neutron flight path of only a few centimeters, placing the neutron production target right inside a  $4\pi$   $\text{BaF}_2$  calorimeter as schematically sketched in Fig. 4. The close geometry implies a gain in neutron flux at the sample position by about three orders of magnitude while keeping all advantages of the calorimeter, such as high efficiency and excellent background discrimination. The two essential features of this arrangement are that the neutron spectrum can be tailored to the specific energy window of astrophysical interest and that the overall experimental time resolution of 1 ns provides still

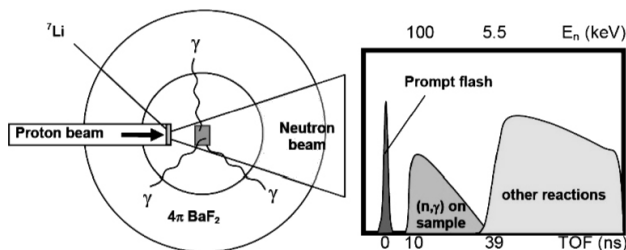


FIGURE 4. Left: Schematic sketch of a proposed setup for measurements on microgram samples using a very close geometry between neutron target and sample. Right: Separation of captures in the sample from  $\gamma$ -backgrounds related to the prompt flash and to neutron interactions with the  $\text{BaF}_2$  scintillator.

sufficient resolution in neutron energy for deriving the required Maxwellian average.

Isotopically pure radioactive samples can be produced either at the upcoming radioactive beam facilities, where the expected intensities suffice to collect the required samples of about  $10^{15}$  atoms in a few hours. In principle, breeding in a high flux reactor or with MeV neutrons is also possible but requires the additional separation of sample and matrix.

## 5. Reactions with charged particles

The nearly 100% efficiency for  $\gamma$ -ray detection makes  $4\pi$   $\text{BaF}_2$  arrays also attractive for measurements of the extremely small cross sections of stellar reactions with charged particles. According to current stellar models,  ${}^{13}\text{C}(\alpha,n){}^{16}\text{O}$  is considered to be the main neutron source for the  $s$  process in AGB stars of 1-3 solar masses. The reaction takes place at temperatures of about  $10^8$  K, which means that the astrophysically relevant energy range for this reaction, the so called Gamov peak, is centered around 190 keV. At this energy a direct measurement of the  ${}^{13}\text{C}(\alpha,n){}^{16}\text{O}$  cross section is extremely difficult. Hence, the experimental data should be pushed to the lowest possible limit to reduce the uncertainties of the extrapolation.

The absolute cross section of the  ${}^{13}\text{C}(\alpha,n){}^{16}\text{O}$  reaction was measured in the energy range  $E_{\text{cm}} = 320 - 700$  keV. While standard techniques are based on the direct detection of the emitted neutrons with  $\text{BF}_3$  and  ${}^3\text{He}$  proportional counters, the new approach made use of the Karlsruhe  $\text{BaF}_2$  array. The  ${}^{13}\text{C}$  target was located inside the  $\text{BaF}_2$  detector, similar to the geometry of Fig. 4, and was surrounded by a converter consisting of a mixture of cadmium powder and paraffin. Neutrons were moderated in the converter and subsequently captured in cadmium. Figure 5 shows that the resulting  $\gamma$ -ray response from neutron capture in the cadmium component of the converter can be well separated from the ambient background due to the higher  $\gamma$  energies and the high event multiplicities. The good signal to background ratio and the very stable operation of the entire setup resulted in fairly

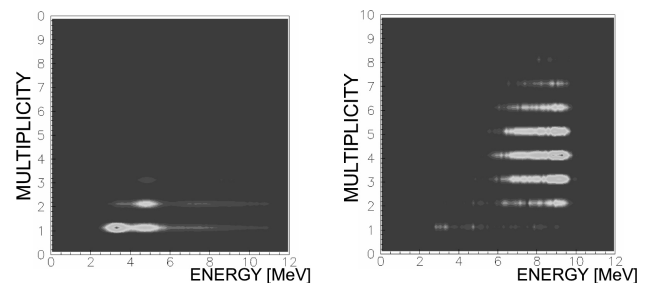


FIGURE 5. The  $\gamma$ -ray energy measured with the  $4\pi$   $\text{BaF}_2$  array as a function of event multiplicity. Left: Ambient background events are characterized by small energies and multiplicities. Right: Neutron captures in the cadmium of the converter exhibit clearly different signatures, resulting in efficient background reduction.

small systematic uncertainties. Accordingly, these results are important for resolving the discrepancies in previous data sets [26].

A second example concerns the measurement of the  $^{12}\text{C}(\alpha, \gamma)^{16}\text{O}$  reaction, one of the key reactions in nuclear astrophysics [27]. In this case, the TOF technique was applied by using a pulsed beam of  $\alpha$  particles from the Karlsruhe Van de Graaff accelerator with a pulse width of 2 ns. In this way backgrounds from  $^{13}\text{C}$  build-up on the sample and from cosmic rays could be significantly reduced by the fast timing of the BaF<sub>2</sub> array.

## 6. Summary

BaF<sub>2</sub>  $\gamma$ -ray calorimeters represent a state-of-the-art approach for a variety of difficult experiments. Their good resolution in  $\gamma$ -ray energy, excellent timing, and large granularity make this type of detectors particularly promising for measurements, where high accuracy and sensitivity are important. In this contribution, these appealing options were illustrated at the example of persisting problems in nuclear astrophysics, but such detectors are also suited for a much wider range of applications, from basic nuclear physics to advanced concepts of nuclear technology.

- 
1. E. Burbidge, G. Burbidge, W. Fowler, and F. Hoyle, *Rev. Mod. Phys.* **29** (1957) 547.
  2. F. Käppeler, *Prog. Part. Nucl. Phys.* **43** (1999) 419.
  3. G. Wallerstein *et al.*, *Rev. Mod. Phys.* **69** (1997) 995.
  4. F. Käppeler, F.-K. Thielemann, and M. Wiescher, *Ann. Rev. Nucl. Part. Sci.* **48** (1998) 175.
  5. M. Busso, R. Gallino, and G. Wasserburg, *Ann. Rev. Astron. Astrophys.* **37** (1999) 239.
  6. E. Anders and N. Grevesse, *Geochim. Cosmochim. Acta* **53** (1989) 197.
  7. W. Aoki *et al.*, *Ap. J.* **580** (2002) 1149.
  8. E. Zinner, *Ann. Rev. Earth Planet. Sci.* **26** (1998) 147.
  9. R. Gallino *et al.*, *Ap. J.* **497** (1998) 388.
  10. C. Travaglio *et al.*, *Ap. J.* **521** (1999) 691.
  11. Z. Bao *et al.*, *Atomic Data Nucl. Data Tables* **76** (2000) 70.
  12. T. Rauscher and F.-K. Thielemann, *Atomic Data Nucl. Data Tables* **75** (2000) 1.
  13. S. Goriely, in *Long term needs for nuclear data development*, edited by M. Herman (International Atomic Energy Agency, Vienna, 2001) report INDC(NDS)-428, p. 83.
  14. K. Wisshak *et al.*, *Nucl. Instr. Meth. A* **292** (1990) 595.
  15. K. Wisshak *et al.*, *Phys. Rev. C* **48** (1993) 1401.
  16. R. Reifarth *et al.*, *Phys. Rev. C* **66** (2002) 064603.
  17. R. Reifarth *et al.*, *Ap. J.* **614** (2004) 363.
  18. P. Lisowski, C. Bowman, G. Russell, and S. Wender, *Nucl. Sci. Engineering* **106** (1990) 208.
  19. U. Abbondanno *et al.*, *Report CERN-SL-2002-053 ECT*, CERN, Geneva, Switzerland (2003).
  20. <http://www.sns.gov/>, Oak Ridge National Laboratory (2004).
  21. <http://j-parc.jp/>, JAERI and KEK (2004).
  22. J. Ullmann *et al.*, in *Capture Gamma-Ray Spectroscopy and Related Topics*, edited by J. Kvasil, P. Cejnar, and M. Kr̄t̄icka (World Scientific, New Jersey, 2003), p. 483.
  23. I. Dillmann *et al.*, n-TOF Note, CERN, Geneva, Switzerland, (2005).
  24. P. Koehler, *Nucl. Instr. Meth. A* **460** (2001) 352.
  25. M. Heil *et al.*, The NCAP proposal, Forschungszentrum Karlsruhe (2005).
  26. M. Heil, *Report FZKA 6783*, Forschungszentrum Karlsruhe (2002).
  27. R. Plag, *Report FZKA 7099*, Forschungszentrum Karlsruhe (2005).